Path Following for Indoor Robots with RFID Received Signal Strength

Ran Liu, Philipp Vorst, Artur Koch and Andreas Zell
University of Tübingen, Department of Cognitive Systems
Sand 1, Tübingen, Germany
E-mail: {ran.liu, artur.koch, andreas.zell}@uni-tuebingen.de

Abstract: **We propose a novel method for robot path following in an RFID-equipped corridor using received signal strength (RSS). RSS measurements are recorded as reference fingerprints during the exploration phase. Then, these data are used to guide the robot through the corridor in the navigation phase. Distance and orientation that the robot derivates from the expected path are approximated through the RSS differences and the index differences of two antennas. Finally, a P-controller is used for the navigation of the robot. This enables the robot to follow a certain path, which may be defined in the first phase of our method. The extensive experiments with a SCITOS G5 service robot confirm the validity and robustness of our approach.**

1. INTRODUCTION

Radio-frequency identification (RFID) is a technology that exchanges data through radio waves between a reader and an electronic tag. The purpose of it is identification and tracking. In the near future, it is possible that RFID technology will appear in our daily lives just like the bar code technology did over the past forty years. RFID tags can be passive (without an internal power supply), active (with an on-board battery) or battery-assisted passive. In this paper, we focus on small and low-cost passive RFID tags, based on the EPC Gen2 standard, which is an international protocol for mostly passive RFID tags.

Our approach demonstrates a path following system with RFID RSS. The method makes no assumptions about the distribution of the RFID tags. Besides that, they are located to the sides of the robot (e.g., on walls of the corridor or goods in shelves). The idea behind our approach is quite simple. It is similar to wall following with laser or line following with vision. In these methods, the orientation and distance of the robot to the wall or the line are computed by different sensors and then passed to a controller to adjust the pose of the robot. However, these approaches rely on expensive hardware configuration or complex processing algorithm. Our approach works as follows: During the exploration phase, the robot is manually controlled to move near the center of a corridor. RFID information is recorded as reference fingerprints during this phase. The term fingerprint in this paper means that the raw sensor data (RFID measurement) represents the location where it is recorded. This was previously used by Vorst *et al.* [4] for robot localization. In the navigation phase, the robot navigates and follows this path automatically by comparing the current fingerprint with the reference fingerprints. The distance from the robot to the expected path is approximated as the RSS differences. The orientation is simplified as the index differences of two antennas in the reference fingerprints. Finally, the RSS difference and orientation are passed to a P-controller, which steers the motors of the robot to navigate in the corridor.

Our proposed method is suitable for UHF RFID tagged environments, such as supermarkets, libraries and logistics centers, where the RFID technology will be possibly widely used in the future. Although, corridor following seems like a limitation of the application of our approach, it should be noted that the supermarkets, libraries, etc. are comprised of corridors. For these environments, RFID navigation is a cost-effective method if the robot is equipped with an RFID system and used for inventory operations or guiding systems.

RFID does not provide any obstacle information. To achieve this one needs to utilize laser range finders, optical sensors or sonar sensors. Note that the focus of this paper is not obstacle avoidance, for which we employ a laser range finder. One may argue that if one already has a laser range finder installed on a mobile robot, thus it is unreasonable to use the much less precise RFID measurements for path following. However, this paper shows it is possible to use RFID fingerprints alone for path following in densely tagged environments, and that this can be done mapless, i.e., without a precise map of the environment.

The remainder of this paper is organized as follows. In Section 2, we give an overview of related work. We present the details of our approach in Section 3, followed by the experimental setup and results in Section 4. We finally draw conclusions in Section 5.

2. RELATED WORK

Due to its inexpensive and contactless identification characteristics, RFID has become an important technology in robotics, and has been employed for different tasks. Previous studies have shown how to use RFID for localization, mapping, navigation and object localization.

Hähnel *et al.* [3] showed for the first time how to localize a mobile robot with RFID. They utilized a probabilistic sensor model for the RFID reader, which computes the likelihood of tag detections given the relative pose of the tag with respect to the robot. Using this model, the positions of passive RFID tags in an office environment were mapped with a highly accurate FastSLAM algorithm. A Monte Carlo approach is finally used to localize the robot. Then, Vorst *et al.* [4] em-

ployed a probabilistic fingerprinting technique to localize a mobile robot accurately in densely tagged environments. Their method requires no explicit sensor model and is capable of exploring given tag infrastructures. Afterwards, Joho *et al*. [6] presented a novel probabilistic sensor model which characterizes RSS information as well as the tag detection to achieve a higher modelling accuracy. They employ this model to localize RFID tags and to track a mobile agent moving through an RFID-equipped environment.

Regarding object tracking with RFID, Deyle *et al.* [10] demonstrated how to produce images of the spatial distribution of RSS for different tagged object environments. They measured the RSS value at each bearing by panning and tilting an RFID reader antenna. The fused ID-specific features derived from an RSS image, a camera image, and a laser range finder scan were used to estimate the tagged objects' 3D locations.

For navigation, Kulyukin *et al.* [1] have shown a wayfinding system for the visually impaired in a structured indoor environment. They employ RFID tags as reliable stimuli that trigger local navigation behaviours to achieve global navigation objectives. Furthermore, Chae *et al.* [2] combine vision and RFID information to localize a robot. The system incorporates an RFID reader on a mobile robot to solve the localization task with respect to a global position. Therefore, a feature matching algorithm is used to validate the local position. However, their method inherits the drawback of vision-based techniques. Moreover, Gueaieb *et al.* [5] proposed a mobile robot navigation technique using phase differences of the received signals from a customized RFID reader. The aim of the navigation algorithm is to make the robot move along virtual paths linking the tags' orthogonal projection points to the ground. The phase difference is then passed to a fuzzy logic controller which provides control actions to the actuators. They achieved their results in simulation. However, a customized RFID reader is needed for their method.

3. APPROACH

3.1 RFID Received Signal Strength

RFID systems are usually comprised of two main components: an RFID reader with antennas, and RFID tags. Passive tags do not contain batteries. Their power is supplied by the reader. When the tags encounter radio waves emitted from the reader, they get power to energize their circuits. The tags then are able to send their encoded data to the reader. Some readers also provide the RSS of each detected tag in dBm, which is the logarithmic expression of received power.

RSS values are heavily influenced by environmental factors and reader antenna setup, such as the reader quality, antenna characteristics, RFID tag properties and transmission power. In our research, the system parameters are already fixed. The environmental factors include the relationship (*e. g.* position and orientation) between the tags and the antenna, multipath propagation, obstacles between the antenna and the tags and the materials that the tags are attached to. In general, it is impossible to model all of these parameters. But RSS values are greatly related to the relative position and orientation of the tag to the antenna, which is the fundamental of this paper.

In order to make the robot navigate in the corridor, our approach comprises two phases: the exploration phase (during which RFID measurement and position data are recorded) and the navigation phase (during which the robot is able to guide itself moving in the corridor by comparing current fingerprints with reference fingerprints).

3.2 Exploration Phase

In the exploration phase, we control the robot moving near the center of a corridor, and record reference fingerprints. Let $F_i=(f_i,p_i)$ be the reference fingerprint at time *i,* which includes an RFID measurement f_i at pose $p_i=(x_i,y_i,\theta_i)$. Furthermore, let A be the number of antennas that are attached to the RFID reader. f_i is a vector, with $f_i=(f_i^{(1)},...,f_i^{(A)})$, which contains A arrays of RSS values of tags that are detected. $f_i^{(a)}=(f_i^{(a,1)},..., f_i^{(a,K)})$, where $a=1,...,A$, K is the total number of tags observed at time *i*. $f_i^{(a,k)}$ is the RSS value of tag k that is detected by antenna a at time *i*. In our configuration, the robot has two antennas, so $A=2$. In addition, (x_i,y_i) are the coordinates of the robot in the global map, and θ_i is the global orientation of the robot. The poses of the robot are computed by a laser range finder. It is important to note that the poses are actually not required for the RFID navigation. They are only used for ground truth measurements and result comparison.

3.3 Navigation Phase

In this phase, the robot follows the path which it travelled in the first phase. Two parameters are needed for the navigation phase: the distance and the orientation deviation to the expected path. In our research, the distance is approximated by the average RSS difference to the reference fingerprints. The orientation is approximated by the index difference in the reference fingerprints of the two antennas. The reference fingerprints with a similarity to the current fingerprint above zero are selected to calculate the RSS difference. Then, a window filter is used to remove the noise of the RSS differences. Afterwards, a particle filter determines the approximated orientation of the robot from the expected path.

3.3.1 Similarity Measurement

To compute the similarity between two fingerprints, we employ a method proposed by Vorst *et al.* [7]. Therefore, the total similarity $sim(g_t,f_i)$ is calculated by a weighted average of the similarity of all antennas $sim(g_t^{(a)}, f_i^{(a)})$:

$$sim(g_t, f_i) = \sum_{a=1}^{A} \frac{n_{max}(g_t^{(a)}, f_i^{(a)})}{\sum_{a=1}^{A} n_{max}(g_t^{(a)}, f_i^{(a)})} sim(g_t^{(a)}, f_i^{(a)}) \quad (1)$$

where $n_{max}(g_t^{(a)}, f_i^{(a)}) = max(|g_t^{(a)}|, |f_i^{(a)}|)$ is the maximum number of detected tags in the lists $g_t^{(a)}$ and $f_i^{(a)}$.

The similarity measure *sim(a,b)* is a symmetric function with non-negative values, which are larger when the two input vectors are more similar. In our experiment, we use the cosine similarity to determine the correspondence between current and reference fingerprints.

$$sim_{cos}(g_t^{(a)}, f_i^{(a)}) = \frac{\sum_{l=1}^{L} g_t^{(a,l)} f_i^{(a,l)}}{\sqrt{\sum_{l=1}^{L} (g_t^{(a,l)})^2} \sqrt{\sum_{l=1}^{L} (f_i^{(a,l)})^2}} \quad (2)$$

3.3.2 Estimation of the RSS Difference

Let H be a list of fingerprints, $H=(H_1, \ldots, H_V)$, which contains V reference fingerprints, whose similarity to the current fingerprint g_t is above zero.

The average RSS difference is computed using the following formula:

$$RSS_{diff}(g_t, F) = \frac{1}{V} \sum_{v=1}^{V} (RSS_{diff}(g_t, H_v)) \quad (3)$$

where $RSS_{diff}(g_t, H_v)$ is the RSS difference between g_t and H_v:

$$RSS_{diff}(g_t, H_v) = \frac{1}{L} \sum_{l=1}^{L} (-1)^a (g_t^{(a,l)} - H_v^{(a,l)}) \quad (4)$$

Since the original RSS difference is very noisy, a window filter is used to smooth the RSS difference.

$$RSS_{smooth}(g_t, F) = \frac{1}{W} \sum_{w=1}^{W} RSS_{diff}(g_{t-w}, F) \quad (5)$$

3.3.3 Estimation of the Orientation

At first, the reference fingerprints are sorted in ascending order by the time when they were recorded. Each fingerprint has a unique index, *1,...,M,* where M is the total number of fingerprints. Then, the orientation that the robot derivates from the expected path is approximated as the difference of the index of left and right antennas in the reference fingerprints. Let $index^{(0)}$ and $index^{(1)}$ be the index of left and right antenna in reference fingerprints respectively, thus the orientation of the robot to the expected path is computed as follows:

$$\theta \approx index^{(0)} - index^{(1)} \quad (6)$$

In this paper, the position of each antenna is estimated by a particle filter. The state of the antenna is expressed by a set of particles $x_t^{(1)}, \ldots, x_t^{(N)}$. They will update over time when the robot moves in a corridor and receives the RFID data. Each particle $x_t^{(n)}$ includes the hypothesis position of the left and the right antenna $x_t^{(n,0)}$, $x_t^{(n,1)}$, and the corresponding weight $w_t^{(n,0)}$ and $w_t^{(n,1)}$. These weights define the associated likelihoods that contribute to the estimation of the positions of the antennas, which are computed by the following formula:

$$index^{(a)} = \sum_{n=1}^{N} x_t^{(n,a)} w_t^{(n,a)} \quad (7)$$

The particle filter algorithm performs three steps recursively: prediction, correction and resampling. In every iteration, each particle is updated according to existing model (predicttion). Then, the particle's weight is modified based on the latest sensor information (correction). Afterward, when a small number of weights dominate the remaining weights, a process called resampling is needed.

1. Prediction:

The position of each antenna at time t is predicted by the previous state and the motion model m_t of the robot.

$$x_t^{(n,a)} = x_{t-1}^{(n,a)} + m_t^{(n,a)} \quad (8)$$

We use a simple motion model

$$m_t^{(n,a)} = s + (-1)^a d \quad (9)$$

where s and d are Gaussian distribution random variables with mean m and deviation v.

2. Correction:

The weight of each particle is updated according to some likelihood function:

$$w_t^{(n,a)} = \eta_t^{(a)} w_{t-1}^{(n,a)} P(g_t^{(a)} \mid x_t^{(n,a)}, m) \quad (10)$$

where $g_t^{(a)}$ is the current observation (in our case, it is the current fingerprint), and m is the representation of the environment. The normalizer $\eta_t^{(a)}$ ensures that:

$$\sum_{n=1}^{N} w_t^{(n,a)} = 1 \quad (11)$$

$P(g_t^{(a)} | x_t^{(n,a)}, m)$ is the observation model. The purpose of the observation model is to find a likelihood function for a particle $x^{(n)}$, given the current measurement g. We compute the likelihood of $p(g|x,m)$ by observing the current fingerprint g from the position $x_t^{(n)}$ for the two antennas individually. Let F be a list of K reference fingerprints whose similarity to the current fingerprint g_t of antenna a is above zero.

$$\begin{aligned} & P(g_t^{(a)} \mid x_t^{(n,a)}, m) \\ &= \sum_{j=1}^{K} P(g_t^{(a)} \mid x_t^{(n,a)}, F_j^{(a)}) P(F_j^{(a)} \mid x_t^{(n,a)}) \\ &= \sum_{j=1}^{K} sim(g_t^{(a)}, F_j^{(a)}) exp(-\frac{1}{2} d(x_t^{(n,a)}, F_j^{(a)}) \end{aligned} \quad (12)$$

where

$$d(x_t^{(n,a)}, F_j^{(a)}) = (x_t^{(n,a)} - F_j^{(a)})^2 \quad (13)$$

3. Resampling:

Resampling is needed when the effective sample size

$$Ess = 1/(\sum_{n=1}^{N} (x_t^{(n,a)} w_t^{(n,a)})^2) \quad (14)$$

drops below a certain threshold. Usually we choose the percentage of the total number of particles, e.g. *N/2*. During resampling, the particles with small weights will duplicate the ones with higher weights. There are many resampling schemes proposed in the literature [9]. In this paper, we employ the residual resampling method presented by Liu *et al.* [8].

3.4 Control Algorithm

The robot used in our experiments utilizes a differential drive. It thus can change its direction by varying the relative speed of two wheels. If both wheels are driven simultaneously at the same speed, the robot moves straight forward. Otherwise, depending on the speed of the wheels, it is able to makes various turns. Thus, the movement of the robot is divided into two independent components: forward speed (v) and rotation speed (ω). For navigation, the forward speed is fixed in this paper. Therefore, the movement of the robot is determined only by R. We use two proportional coefficients ($P= [K_o,K_r]$), as shown in formula (15) to combine the orientation and RSS difference together to make the robot follow the path at the first stage.

$$\omega = P \cdot [\theta, RSS_{smooth}]^T = K_o\theta + K_r RSS_{smooth} \qquad (15)$$

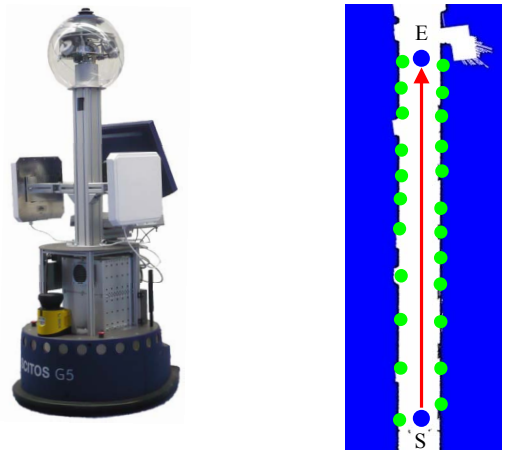

Fig. 1. Left: The experimental platform: a SCITOS G5 service robot with its UHF RFID antennas spanning an angle of approx. 180°. Right: Map of the experimental environment. RFID tags were attached on each side of the corridor. Blue circle: the robot; green circles: the RFID tags; red line: the ground truth of exploration phase; S: the start position of the robot; E: the end position of the robot.

4. EXPERIMENTAL RESULTS

We conducted several experiments with a Metralabs SCITOS G5 service robot. Our robot is equipped with a laser range finder (SICK S30B-2011DA, 270° field of view), and an Impinj®, Inc., Speedway Gen. 2 UHF RFID reader (865 MHz-956 MHz), as shown in Fig. 1. The reader features a maximum RSS sensitivity of -80 dBm. It is connected to two circularly polarized antennas by Laird Technologies (type S8688PL,S8688PR, 865 MHz-870 MHz, about 8.5 dBi antenna gain), and offers a maximum read range of 7 meters. The scan in the XY plane spans an angle of approx. 180^0.

The environmental setup of our experiment is shown in Fig. 1. It is comprised of a corridor (2.6 meters width and 35 meters long). We placed passive RFID tags (type Alien Technology Squiggle, ISO/IEC 1800-6C) at both sides of the corridor at a distance of approx. 1m. The height was about 0.8 meters, nearly the same height as the RFID antennas.

We controlled the robot to record a number of reference fingerprints in the corridor, where a total of 95 tags were placed. The maximum speed of the robot was set to 0.3m/s, and the RFID reader worked at a sampling period of 0.5s. This corresponds to a total of 260 fingerprints. To confirm the effectiveness of our algorithm, the tests were performed with varied parameters, like different speeds/sample periods and initial robot poses.

The ideal parameters of P-controller in our experiments depend on the RFID sample period and the maximum robot speed that the reference fingerprints were recorded at. They also rely on the forward speed during the navigation phase. We needed several trials to adjust the P parameters (nearly 4 trials, which usually took 5 minutes) if the environmental set-up was changed. In our experiments, the maximum robot speed and RFID sample period are fixed during the exploration phase. Therefore, we set $P_1 = (K_o, K_r) = (0.008, -0.06)$.

4.1 Influence of Particle Filter Parameters

4.1.1 Dfferent Particle Numbers

In this section, we investigate how the number of particles influences the performance of orientation tracking in our algorithm. We remotely controlled the robot to rotate quickly for a certain angle, and stopped it for several seconds. We repeated this several times and logged the RSS as the tested benchmark. Finally, we applied the particle filter with variable number of particles to observe the performance of our algorithm.

Our algorithm is running on an Intel Pentium 4 CPU, 2.6 GHz. The index differences with different particle numbers and the actual orientation of the robot are shown in Fig. 2. The run times are shown in Tab. 1. It is obvious that the largest number of particles achieves the best tracking results. It is much faster to track the orientation changes, but it also costs more run time. The tracking abilities of 100 particles, 500 particles and 2000 particles do not have so much difference, but the run times increase rapidly (1.8ms, 5.6ms and 19.5ms correspondingly). Therefore, we choose 500 particles for the navigation in our algorithm.

Table 1: Mean run times of the particle filter for different particle numbers.

Number of particles	10	100	500	1000	2000
Run time(ms)	1.0	1.8	5.6	10.4	19.5

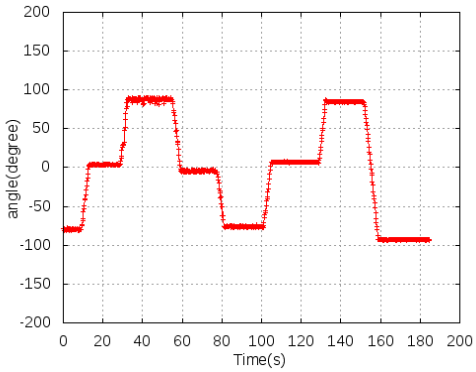

(a)

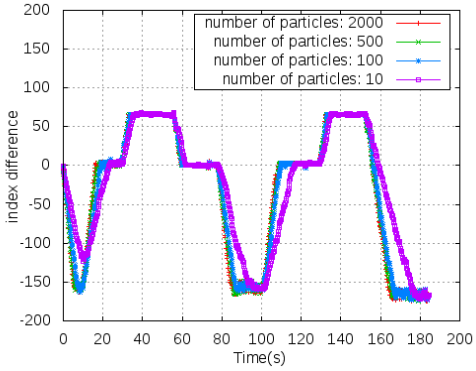

(b)

Fig. 2. Impact of the number of particles on the performance of orienttation tracking. (a) Actual orientation of the robot. (b) Index difference using various numbers of particles.

4.1.2 Influence of Different Motion Models

The impact of the robot's motion model was examined in the next experiment. We modified the values of the standard deviation for the Gaussian random to examine the orientation tracking capability of the particle filter. We used the same log files as in the previous stage (Sect. 4.1.1). Fig. 3 shows the results under different deviation levels. It can be seen that the particle filter with large deviations is more sensitive to the change of orientation, but also has a lot of noise. In con-trast, the response of small deviations is slower, but much smoother. Thus, a deviation of 1.0 is selected to guide the robot in the corridor in our algorithm.

4.2 Performance of the Robot Navigation

4.2.1 Different Initial Poses

In order to confirm the effectiveness and robustness of our proposed algorithm, we did experiments by placing the robot at different initial positions and orientations in the corridor.

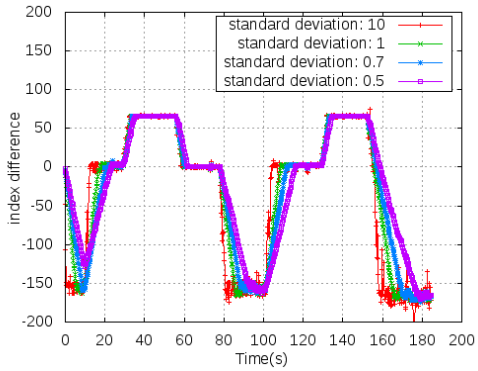

Fig. 3. Influence of the motion model with different standard deviations of Gaussian random.

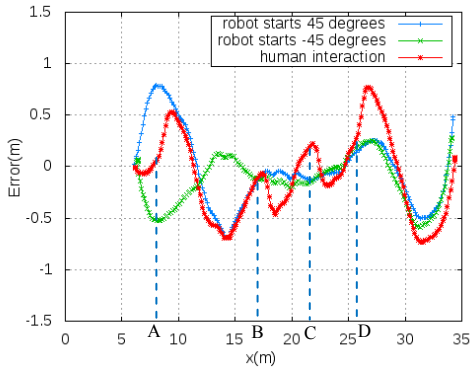

(a)

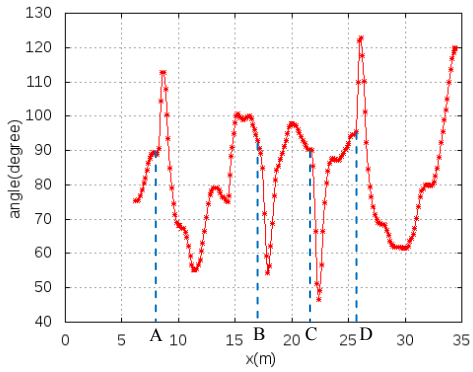

(b)

Fig. 4. Influence of different initial orientations on the navigation of the robot. (a) Tracking errors. (b) Actual orientations of the robot under human interaction.

A. Different Initial Orientations

As shown in Fig. 4, the robot started approximately at the center of the corridor with initial orientations of nearly 45° and -45° to the expected path. The experiments show that the robot is capable of navigating through the corridor regardless of the initial angles. To further test the stability of our algorithm, we added some human interactions while the robot navigated through the corridor (see in Fig. 4). The orientation of the robot was altered with sudden disturbances at positions A, B, C, and D (nearly 40°). The results show that the robot is

able to detect the changes in orientation quickly, and ad-justs its heading back to the expected path. Also, it can be seen that the navigation does not converge. An explanation for this is that the PID controller relies on input of the mea-surement and is poor to deal with the noise. Although a win-dow filter and a particle filter are used to smooth the RSS measurement, the noise still exists.

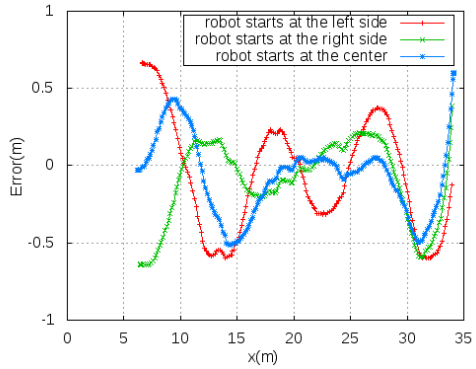

Fig. 5. Tracking errors of different initial positions for the navigation of the robot.

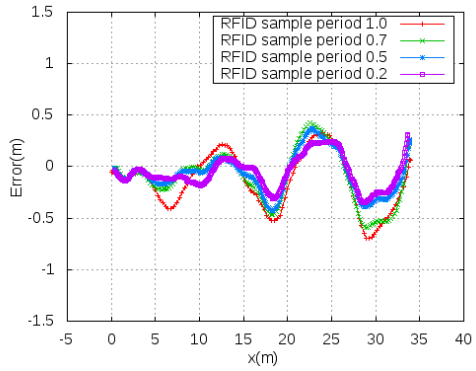

(a)

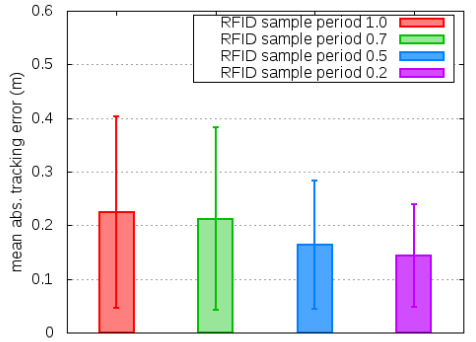

(b)

Fig. 6. Influence of different sample periods on the navigation of the robot. (a) Tracking errors. (b) Means and standard deviations of tracking errors.

B. Different Initial Positions

In another experiment, the robot started at the left and right sides of the corridor with an initial orientation of nearly 0 degrees as shown in Fig. 5. The results demonstrate that our algorithm has the ability to guide the robot along the expected path irrespective of its initial position.

4.2.2 Different RFID Sample Periods

The influence of various RFID sample periods was investigated in the next experiment, as shown in Fig.6. In this experiment, the robot started at nearly the same pose, and moved at a maximum speed of 0.3 m/s. We measured the mean and standard deviations of absolute tracking errors (see Fig. 6 (b)). The results show that lower sample periods (i.e., high sample frequencies) lead to smoother trajectories and lower absolute tracking errors. This is natural since the response of lower sample period is faster. With a low sample period of 0.2s, the robot can achieve a mean absolute tracking error of 0.14m.

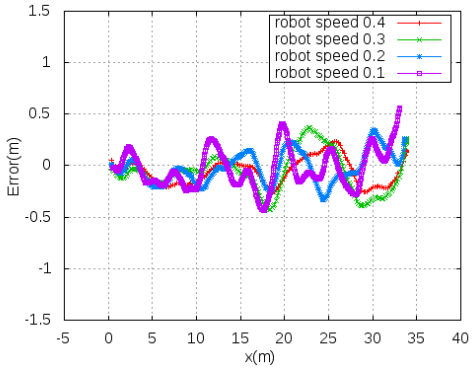

(a)

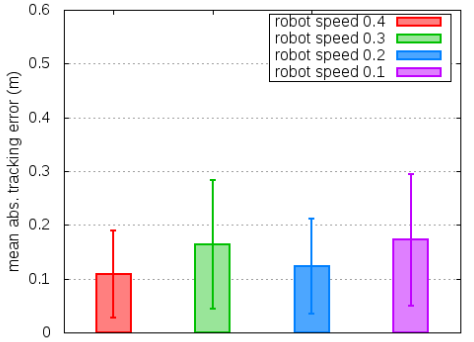

(b)

Fig. 7. Influence of different speeds on the navigation of the robot. (a) Tracking errors. (b) Means and standard deviations of tracking errors.

4.2.3 Influence of the Robot Speeds

The impact of the robot speed was examined in the last experiments. The robot was placed at nearly the same pose, the RFID sample period was set to 0.5s. The results are shown in Fig. 7. As can be seen lower speeds result in oscillated trajectories. This is due to the parameters of P-controller for low speed (0.1 m/s). To confirm this, we conducted another ex-

periment with different value of P at a speed of 0.1m/s, as shown in Fig. 8. This experiment shows a large P leads to oscillation of the navigation. On the other hand, a small value results in smooth trajectory, but less sensitive to deal with the orientation and distance changes. This is obvious for a P-controller that a high proportional coefficient results in a large change in the output for a given change in the input, thus the system can become unstable. A small coefficient, by contrast, leads to a small response, and a less responsive or less sensitive controller. With a $P=30\%P_1$, the robot is able to achieve a mean absolute tracking error of 0.08m.

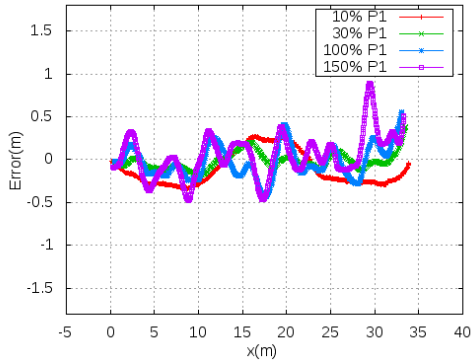

(a)

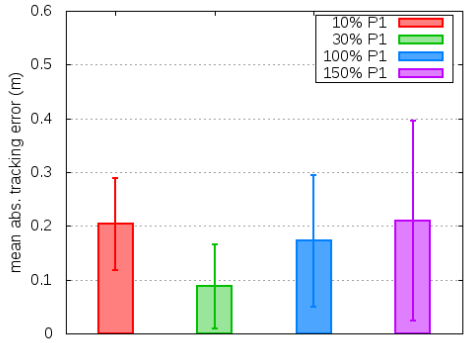

(b)

Fig. 8. Influence of different parameters of P-controller on the navigation of the robot. (a) Tracking errors. (b) Means and standard deviations of tracking errors.

5. CONCLUSION

5.1 Summary

This paper shows that it is possible for a mobile robot to follow a learned path in a corridor using only passive UHF RFID data with RSS, assuming a tag density of at least 1/m. This is possible despite the rather long maximum read range of 7m of RFID reader, which is much larger than the corridor width (2.6m). To achieve this, we firstly manually control the robot move through the corridor once close to the center line, and then the robot will navigate through the corridor automatically. At a robot speed of 0.3m/s and low RFID sample period (0.2 s) (i.e., high RFID sample frequency 5HZ), our method achieves an accuracy of navigation errors ±0.07m. Our algorithm provides a computationally simple, easily implemented and cost-effective alternative to other corridor navigation techniques for indoor robots.

5.2 Future Work

In the future, we plan to investigate how tag density and tag height influence the navigation of the robot. We are going to employ some smart control algorithms, such as fuzzy logic or adaptive controls to optimize our algorithm. Finally, we want to apply our approach in large-scale environments like supermarkets or libraries to verify the robustness.

REFERENCES

[1] V. Kulyukin, C. Gharpure, J. Nicholson, and G. Osborne, Robot-Assisted Wayfinding for the Visually Impaired in Structured Indoor Environments, *Autonomous Robots*, 21(1), pp. 29-41, 2006.

[2] H. Chae and K. Han, Combination of RFID and Vision for Mobile Robot Localization, In *Proc. of the 2005 Int. Conf. on Intelligent Sensors*, pp. 75-80, 2005.

[3] D. Hähnel, W. Burgard, D.Fox, K. Fishkin, and M. Philipose, Mapping and Localization with RFID Technology, In *Proc. of the 2004 IEEE Int. Conf. on Robotics and Automation (ICRA)*, pp. 1015-1020, 2004.

[4] P. Vorst, S. Schneegans, B. Yang, and A. Zell, Self-localization with RFID Snapshots in Densely Tagged Environments, In *Proc. of the 2008 IEEE/RSJ Int. Conf. on Intelligent Robots and Systems (IROS 2008)*, pp. 1353-1358, Nice, France, September, 2008.

[5] W. Gueaieb, and M. S. Miah, A Modular Cost-Effective Mobile Robot Navigation System Using RFID Technology, *Journal of Communications*, 4(2), pp. 89-95, March, 2009.

[6] D. Joho, C. Plagemann, and W. Burgard, Modeling RFID Signal Strength and Tag Detection for Localization and Mapping, In *Proc. of the 2009 IEEE Int. Conf. on Robotics and Automation (ICRA)*, pp. 3160-3165, Kobe, Japan, May, 2009.

[7] P. Vorst and A. Zell, A Comparison of Similarity Measures for Localization with Passive RFID Fingerprints, In *ISR/ROBOTIK 2010 (Proc. of the Joint Conf. of ISR 2010 (41st Int. Symposium on Robotics) and ROBOTIK 2010 (6th German Conf. on Robotics))*, pp. 354-361, VDE Verlag, June, 2010.

[8] J. S. Liu and R. Chen, Sequential Monte Carlo Methods for Dynamic Systems, *Journal of the American Statistical Association*, vol. 93, no.443, pp. 1032-1044, 1998.

[9] R. Douc, O. Cappe, and E. Moulines, Comparison of Resampling Schemes for Particle Filtering, In *Proc. of the 4th Int. Symposium on Image and Signal Processing and Analysis*, pp. 64-69, 2005.

[10] T. Deyle, H. Nguyen, M. Reynolds, and C. C. Kemp, RF Vision: RFID Receive Signal Strength Indicator (RSSI) Images for Sensor Fusion and Mobile Manipulation, In *Proc. of the 2009 IEEE/RSJ Int. Conf. on Intelligent Robots and Systems (IROS)*, pp. 5553-5560, October, 2009.